Transactions of the SMiRT 27
Yokohama, Japan, March 3-8, 2024
Division V

PARAMETRIC EVALUATION OF PCCV INTERNAL PRESSURE CAPACITY VIA SECTIONAL ANALYSIS

Thomas Kang[1], Seung Heon Lee[2], Christopher Jones[3], Javeed Munshi[4]

[1] Seoul National University, Seoul, South Korea (tkang@snu.ac.kr)
[2] Seoul National University, Seoul, South Korea
[3] Kansas State University, Manhattan, KS, USA
[4] Bechtel, Reston, VA, USA

ABSTRACT

The internal pressure capacity of a prestressed concrete containment vessel (PCCV) is crucial to its role as the final barrier in the defense-in-depth system. In this study, a sectional analysis approach is utilized to estimate the internal pressure capacity of a 1:4 scale PCCV specimen according to the global free-field strain criteria provided by USNRC Regulatory Guide 1.216. The result of this analysis is expanded to the probabilistic realm based on the methodology presented by Tang et al. (1995), where an equivalent peak liner strain is compared with a liner strain criterion. Failure probabilities according to internal pressure are constructed for several liner strain criteria, and the best estimate, upper bound, and lower bound are obtained for each case. Thereafter, a parametric evaluation is performed for internal pressure capacity according to two factors: the level of prestressing and usage of fiber reinforced concrete (FRC). Results provide insights into the optimization of PCCV internal pressure capacity.

INTRODUCTION

The key role of a prestressed concrete containment vessel (PCCV) is to maintain functional and structural integrity under various severe accident scenarios as the final barrier in a nuclear power plant's defense-in-depth system. In particular, the pressure capacity of a PCCV refers to the maximum beyond design-basis internal pressure at which the containment retains both its functional and structural integrity (NRC 2010), and whose threshold is typically expressed as designated failure criteria.

Currently, the commercial viability of concrete containments is being challenged in the market due to high initial costs, which calls for optimizations in PCCV performance where internal pressure capacity is one of the primary facets. However, it is difficult to capture trends according to diverse design parameters if high fidelity finite element analyses (FEAs) are conducted on a case-by-case basis. In this study, sectional analysis is performed on a 1:4 scale PCCV model via the strain compatibility method, to obtain a reasonable estimate on its deterministic internal pressure capacity. This method is expanded to the probabilistic realm by referring to the methodology presented by Tang et al. (1995) which provides a probabilistic framework based on liner tear criteria. These methods are implemented in a parametric study with two factors: the level of prestressing and usage of fiber reinforced concrete (FRC). Throughout this study, the effects of various design parameters are discussed and areas for further research are identified.

BACKGROUND

In evaluating the internal pressure capacity, NUREG/CR-6906 defines two failure modes for PCCVs subject to beyond design-basis quasi-static internal pressure: functional and structural failure modes. Functional failure is defined as a loss of containment function, i.e., a loss of function as a leaktight pressure boundary as it exceeds a specified leak rate. In a mechanistic sense, functional failure is typically preceded by global yield of the containment structure or local material failure at discontinuities. Structural failure is

defined as the global loss of capacity in the containment structure to resist the applied loads, which potentially leads to catastrophic rupture and uncontrolled release of fission products.

The global yield and failure of a nuclear containment vessel is largely governed by the global hoop strains at the midheight of the cylinder due to its one-directional curvature. Hessheimer and Dameron (2003) report that global, free-field hoop strains on the order of 0.5 to 1.0% can be achieved before functional and structural failures for PCCVs, respectively. The main experimental basis for this observation is the 1:4 scale model overpressurization test conducted by Sandia National Laboratories in 2000~2001, whose data was extensively documented and made publicly available (Hessheimer et al. 2003), as well as having been extensively studied in subsequent research projects (NEA 2005, Heitman et al. 2014).

Based on these previous endeavors, USNRC Regulatory Guide 1.216 (RG 1.216) provides global strain-based failure criteria for PCCVs, where the following limits are given: (1) a total tensile average strain in tendons away from discontinuities of 0.8%, and (2) a global free-field strain for the other materials that contribute to resist the internal pressure (i.e., liner, if considered, and rebars) of 0.4%. This criteria essentially takes the global free-field strain as a surrogate parameter for leak rate, and seems to assign a conservative estimate of the aforementioned 0.5% strain which corresponds to the functional failure mode.

While RG 1.216 provides a basis for the deterministic evaluation of a PCCV's internal pressure capacity, there has yet to be definitive regulatory guidance for probabilistic assessments. However, some of the available literature provide theoretical frameworks for probabilistic evaluations, one of which is the research project sponsored by the Electronic Power Research Institute (EPRI) in the late 1980s-1990s. Here, the global liner strain ε_{glo} is multiplied by a biaxiality factor B and a strain concentration factor K to obtain the equivalent peak strain ε_{peak} and then compared to strain-based liner tear criteria. The B and K factors were evaluated experimentally, and 5 sets of B and K factors curves with respect to global liner strain were developed in the EPRI program for typical locations of PCCV liners (Heitman et al. 2014).

The methodology assumes that ε_{glo}, B and K are independent lognormal random variables, each assigned with randomness and uncertainty ranges (Tang et al. 1995). It goes to follow that ε_{peak} also follows a lognormal distribution, and the probability of liner tear for a strain criterion can be obtained for each step of internal pressure. Tang et al. (1995) further developed this approach by quantifying liner tear size and leak rates to obtain failure probability graphs for different failure sizes; however, such formulations require integrations across the entirety of a PCCV. For the scope of this study, deterministic strain-based criteria are taken, and corresponding failure probabilities with respect to internal pressure are obtained.

METHODOLOGY

Strain Compatibility Method

The strain compatibility method (SCM) is an analytical approach most often utilized for reinforced concrete (RC) beams. It is based on the principle that in a composite material like RC, both concrete and steel reinforcement must experience the same strain under loading conditions. The method assumes that plane sections remain plane, and involves determining a linear strain distribution of a cross section whose corresponding stress distribution satisfies equilibrium with external load effects.

In this study, SCM is utilized for the SNL 1:4 scale PCCV model with axisymmetric assumptions (Figure 1) to obtain a reasonable estimate of the global hoop strain, which is the primary driver of the limit state (Dameron et al. 2003). As there is no distinction in behavior for bonded and unbonded hoop tendons under axisymmetric assumptions, strain compatibility can be assumed for the prestressing steel. Poisson's effects due to the vertical tensile force are ignored because the primary load resisting elements (prestressing steel and rebar) exhibit one-directional behaviors. The assumed stress-strain relationships are depicted in Figures 2(a) to (e), where the material properties are determined from test results presented by Hessheimer

et al. (2003). An initial prestressing of f_{se} = 889 MPa is assumed (Figure 2(f)), which counteracts 1.2~1.3 times the design pressure P_d = 0.39 MPa.

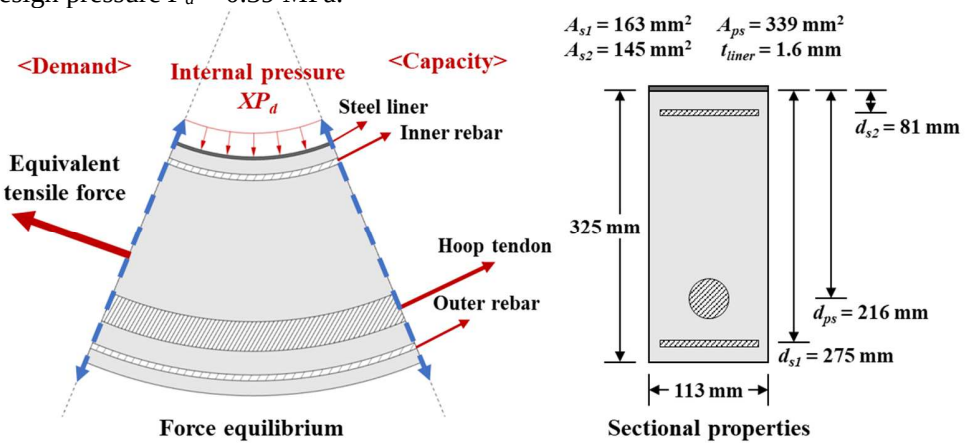

Figure 1. Diagram for strain compatibility method

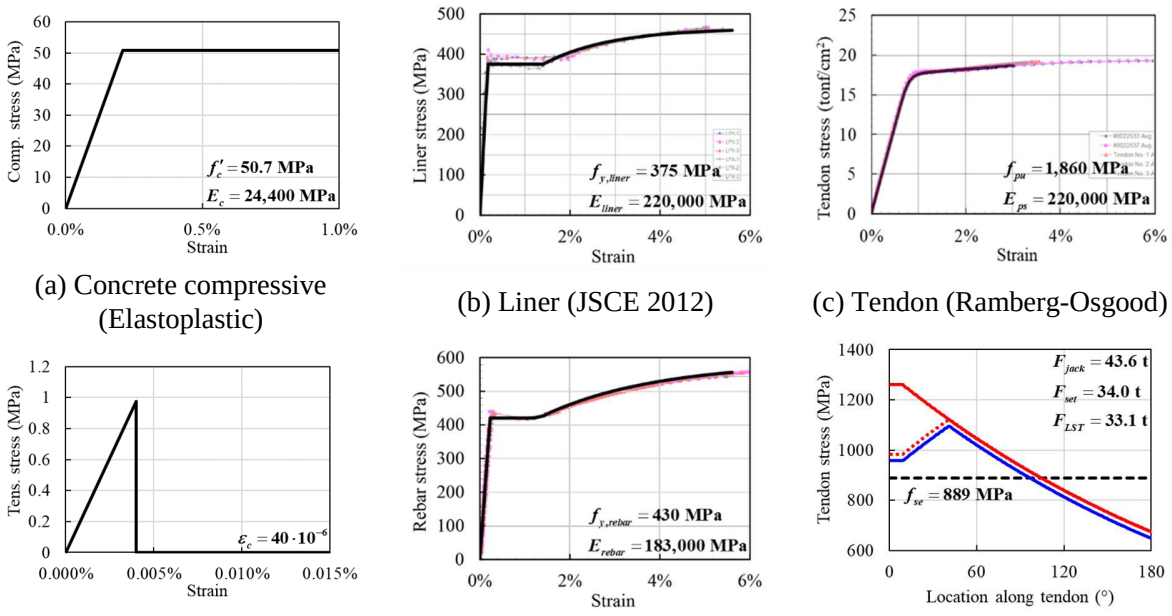

(a) Concrete compressive (Elastoplastic)
(b) Liner (JSCE 2012)
(c) Tendon (Ramberg-Osgood)
(d) Concrete tensile (Brittle)
(e) Rebar (JSCE 2012)
(f) Tendon stress distribution

Figure 2. Material properties assumed for SCM

Figures 3(a), 3(b), and 3(d) compare the results of the SCM to the experimental and analytical data provided in NUREG/CR-6809, each denoted as 'Sectional Analysis,' 'Experiment,' and '2000 Analysis,' respectively. The data for radial displacement, liner hoop strain and outer rebar hoop strain are taken from the 135-degree azimuth as a representative value for global free-field response. As the RG 1.216 criterion for tendons evaluates the average strain instead of a designated point, Figure 3(c) compares SCM results to strain data taken from various measurement points across Tendon H68 of the experiment, reasonably far from the equipment hatch (Hessheimer et al. 2003). The following observations can be made:

- Radial displacement obtained from SCM generally agrees well with the established data, but is slightly overestimated up to the cracking of concrete near $1.5P_d$. This initial deviation is likely due to the neglected Poisson's effect where the compressive vertical stress incurs tensile hoop strain. However, its influence quickly diminishes at beyond design basis internal pressure.

- Liner and rebar hoop strains generally agree well with the analytical results, but the results of SCM enter the plastic phase entirely after global yield, whereas analysis results yet exhibit a marginal increase in load capacity. This is possibly due to the additional stiffness provided by the extra wall thickness and steel reinforcement at buttresses and penetrations.
- Experimental data for liner and rebar hoop strain show decreased stiffness around 0.2%. For the rebars, NUREG/CR-6809 attributes this to an inherent overestimation in the instrumentation due to the grinding at gage installation points. In the case of the liners, the amplified strain is attributed to local details or loss in compatibility due to adjacent concrete cracks. In the context of taking global behavior as a predictive measure for failure, however, conformity with analytic results takes precedence over local strain concentrations, as long as the radial displacement in the experiment is correctly predicted.
- Hoop strains obtained from SCM reach the 0.4% threshold at $3.22P_d$ (1.25 MPa) for the liner and $3.23P_d$ (1.26 MPa) for the outer rebar. Between the two sets of data, SCM results for the liner will always govern for the 0.4% strain criteria, as the inner strain of a cylindrical shell is always larger than the outer strain under axisymmetric expansion or contraction.
- The tendon hoop strain obtained from SCM generally agree well with the experimental data, although the transition to plastic phase would likewise result in a slight strain overestimation. The strain reaches the 0.8% criteria at $3.18P_d$ (1.24 MPa), meaning that the tendon hoop strain governs in determining the internal pressure capacity of the PCCV model. This is because the initial tensile strain due to post-tensioning is above 0.4%, and the total strain therefore reaches 0.8% before the liner strain gets to 0.4%. Conversely, the liner strain would govern if the level of prestressing is lower.

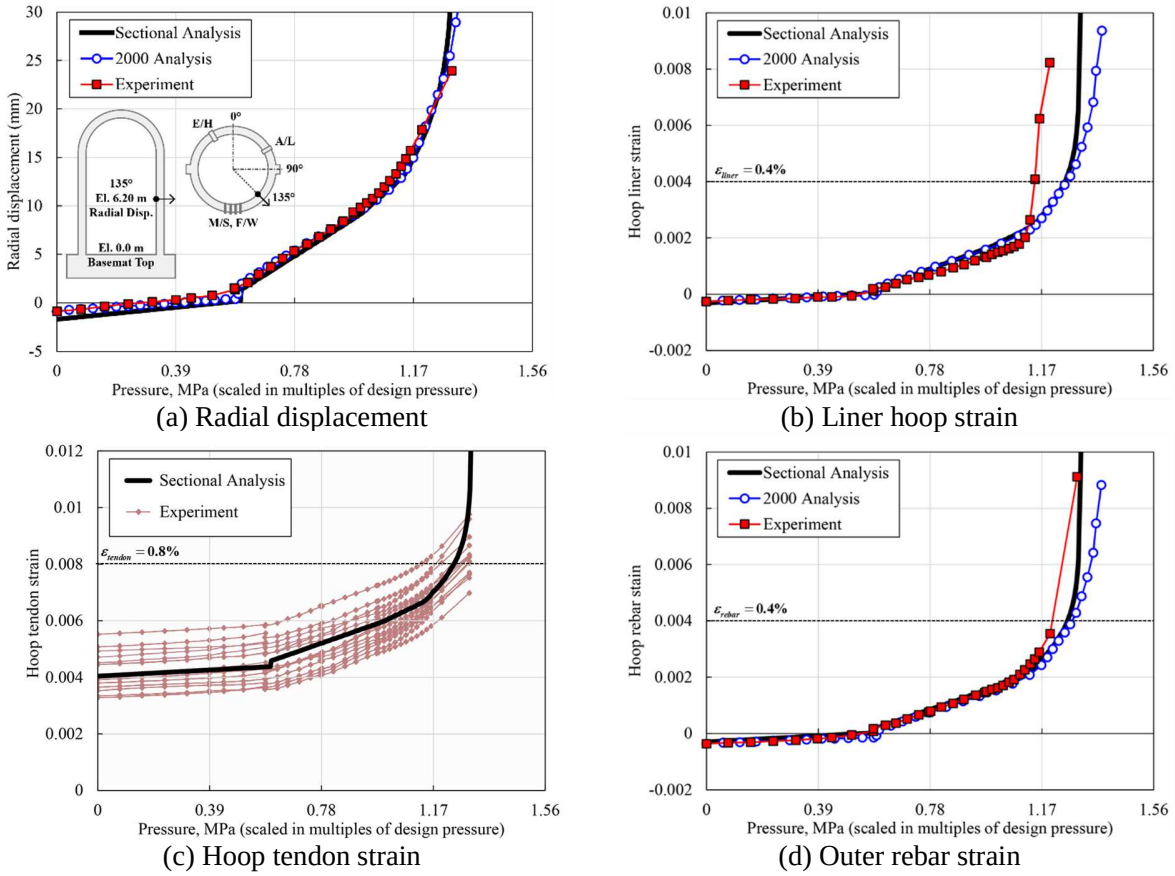

(a) Radial displacement (b) Liner hoop strain

(c) Hoop tendon strain (d) Outer rebar strain

Figure 3. Comparison of SCM results to experimental and analytical data

Probabilistic Evaluation of Internal Pressure Capacity

Based on global liner hoop strain obtained from the SCM, the internal pressure capacity of the PCCV is probabilistically evaluated using the EPRI methodology detailed by Tang et al. (1995). This methodology obtains global liner strains via 2D axisymmetric analysis and multiplies them by biaxiality factor *B* and strain concentration factor *K* to obtain an equivalent peak strain, i.e.,

$$\varepsilon_{peak} = BK\varepsilon_{glo} \tag{1}$$

Where: ε_{peak}, ε_{glo}, *B* and *K* are values of the peak strain, global strain, biaxiality factor and strain concentration factor at a specified internal pressure.

In this theoretical framework, the three parameters ε_{glo}, *B* and *K* are treated as random variables with lognormal distributions, as:

$$\varepsilon_{glo} = \hat{\varepsilon}_{glo}\gamma_u\gamma_R \tag{2}$$

$$B = \hat{B}\xi_u\xi_R \tag{3}$$

$$K = \hat{K}\lambda_u\lambda_R \tag{4}$$

Where: $\hat{\varepsilon}_{glo}$, $\hat{B}$, and $\hat{K}$ are the deterministically assigned values of global strain, biaxiality factor and strain concentration factor, and γ_u, γ_R, ξ_u, ξ_R, λ_u, and λ_R are lognormally distributed variables with median unity and dispersions β_u and β_R.

Randomness and uncertainty are quantified as the dispersions (i.e., logarithmic standard deviations), whose values are taken from Tang et al. (1995) and shown in Table 1. As ε_{peak} is also a lognormally distributed variable, its dispersion β_c can be expressed as the square root of the sum of squares of the individual dispersion values. Based on the EPRI database, the $\hat{B}$ and $\hat{K}$ factors are taken as the mean values of the following cases relevant to midheight response: 1) equipment and personnel hatches, 2) steam line and other penetrations, and 3) locations where embedded angle anchorages terminate (Figure 4). It can be seen that the mean biaxiality factor reaches a value of 1.76 and the strain concentration factor has a value of 23.6 at the RG 1.216 failure criteria of 0.4%, i.e., the onset of global yielding. The $\hat{K}$ factor graph in relation to the 0.4% strain is consistent with the remark by Tang et al. (1995) that *K* reaches an initial peak at the point of localized yield, after which it declines as the yield area propagates up to a global yield state.

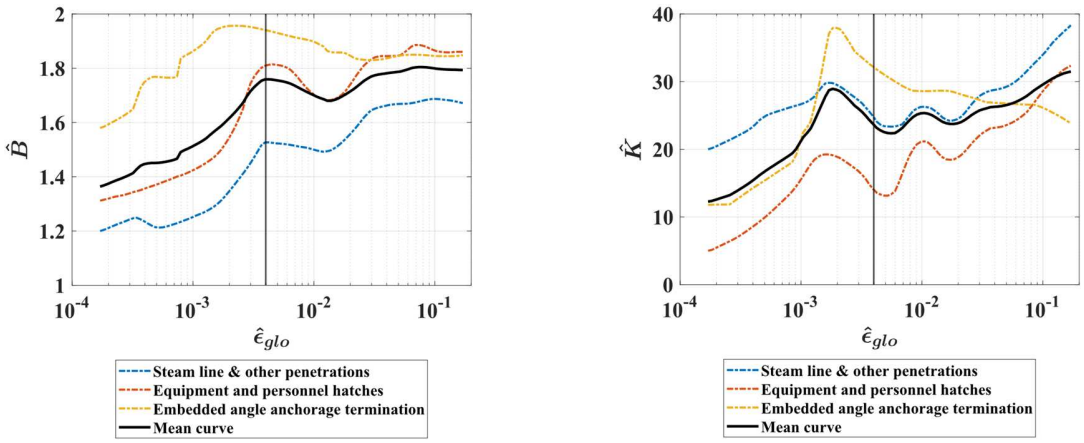

(a) Biaxiality factor $\hat{B}$ (b) Strain concentration factor $\hat{K}$

Figure 4. $\hat{B}$ and $\hat{K}$ factors for steam line and other penetrations in PCCVs (Tang et al. 1995)

Table 1. Representative values for randomness and uncertainty

	ε_{glo}	B	K
β_u	0.15	0.10	0.10
β_R	0.05	0.16	0.05
$\sqrt{\beta_u^2+\beta_R^2}$	0.158	0.189	0.112
β_c	0.27		

The baseline failure criterion is taken as a peak liner strain of 34% determined from uniaxial coupon tests (Dameron et al. 2000). It should be noted that NUREG/CR-6685 assumes a liner tear strain of 18.5%, which is the 34% strain modified to account for biaxiality; as this study implements biaxiality via the *B* factor, the 34% criteria is deemed suitable. NUREG/CR-6685 also introduced a knockdown factor of 0.6 for liner steel adjacent to welds, to account for gage effects emerging from lack of deformation in the welding material. This would reduce the failure criterion to an order of 20%. Furthermore, NUREG/CR-6810 states that the numerous weld repairs in the PCCV model reduced the liner thickness, by up to 40% in severe cases. This was an artifact of scaling weld acceptance criteria to the 1:4 model (Hessheimer et al. 2003), and detailed analyses in NUREG/CR-6809 show that strain concentration factors can reach up to $\hat{K}=91$ at 0.4% global strain, i.e., 3.9 times the $\hat{K}=23.6$ assumed for this study. This corresponds to a failure criterion on the order of 34%/3.9 ≈ 9% strain. The three strain criteria of 34%, 20%, and 9% are depicted alongside the median peak strain $\hat{\varepsilon}_{peak}$ and the 95% confidence interval curves in Figure 5(a).

Figure 5(b) plots the probabilities of failure according to internal pressure by computing $P(\varepsilon_{peak}/\varepsilon_{failure}>1)$ for the lognormally distributed variable ε_{peak} with dispersion β_c = 0.27 and the peak strain criteria $\varepsilon_{failure}$ = 34%, 20%, and 9%. Additionally, probabilities of failure are depicted for the global liner strain ε_{glo} with dispersion $\sqrt{\beta_u^2+\beta_R^2}$ = 0.158 and $\varepsilon_{failure}$ = 0.4%, 0.5%, and 1%, which correspond to the RG 1.216 failure criterion for liners and global free-field strain at functional and structural failures, respectively (Hessheimer and Dameron 2006). The lower bound, best estimate, and upper bounds given in Table 2 are taken as the 10th, 50th, and 90th percentiles of the probability curves. The following observations are made:

- The 34% peak strain criterion results in a probability curve similar to the 1.0% global strain criterion for structural failure, and is likely not indicative of the "weak links" in the entire liner that would govern initial tearing.
- The 20% peak strain criterion shows a best estimate and an upper bound similar to the 0.5% global strain criterion, and a lower bound similar to the 0.4% global strain criterion. As the 20% peak strain criterion approximately coincides with the global strain criteria, the right side of the probability curve is distinctly steeper compared to the left, mirroring deterministic trends near global yield.
- The 9% peak strain criterion results in a probability curve with a gentle slope, and where failure occurs at significantly lower pressure levels than the other criteria. The upper and lower bounds encompass the $2.5P_d$, corresponding to the 20th percentile, at which initial liner tearing occurred for the PCCV model experiment. However, as the 9% criteria is primarily an artifact of the 1:4 scaling, it would be reasonable to set a liner tear criterion between 9% and 20% for a real-scale PCCV, i.e., assign knockdown factors between 0.25~0.6 to the ultimate strain measured from uniaxial coupon tests.
- Compared to the RG 1.216 failure criteria, implementing the EPRI methodology has the benefit of being able to quantify the effects of discontinuities, weld seams, or flaws in the liner and implement them into a probabilistic framework. However, this approach only depicts failure in terms of the liner strain and cannot reflect the 0.8% tendon failure criterion of RG 1.216. If the methodology were to be further developed, it would be desirable to formulate a framework for tendon failure and obtain the probability of the union of liner and tendon failures.

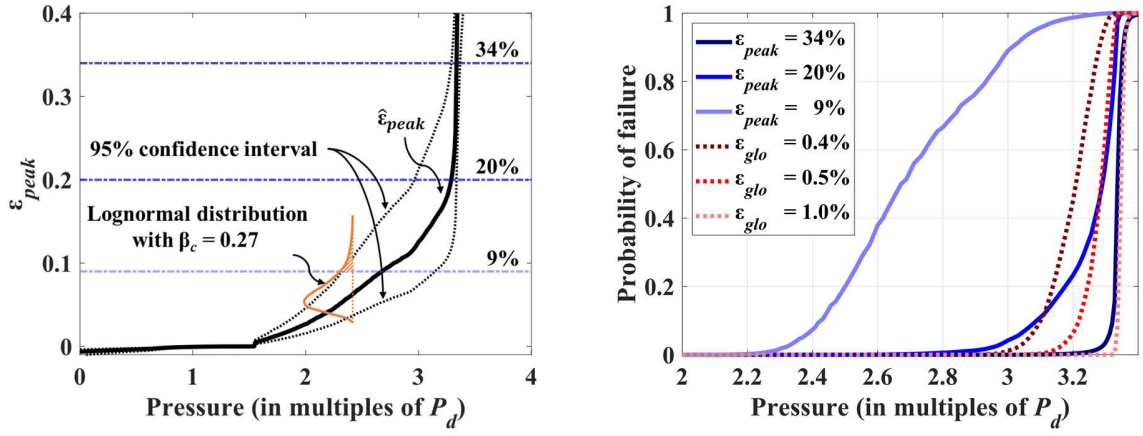

(a) Peak liner strain ε_{peak} (b) Probability of failure

Figure 5. Probabilistic evaluation procedure

Table 2. Failure probability according to strain criteria

	Lower bound	Best estimate	Upper bound
ε_{peak} = 34%	3.32P_d (1.29 MPa)	3.34P_d (1.30 MPa)	3.35P_d (1.31 MPa)
ε_{peak} = 20%	3.09P_d (1.20 MPa)	3.29P_d (1.28 MPa)	3.33P_d (1.30 MPa)
ε_{peak} = 9%	2.42P_d (0.95 MPa)	2.67P_d (1.04 MPa)	3.02P_d (1.18 MPa)
ε_{glo} = 0.4%	3.10P_d (1.21 MPa)	3.21P_d (1.25 MPa)	3.28P_d (1.28 MPa)
ε_{glo} = 0.5%	3.22P_d (1.25 MPa)	3.29P_d (1.28 MPa)	3.32P_d (1.29 MPa)
ε_{glo} = 1.0%	3.34P_d (1.30 MPa)	3.34P_d (1.30 MPa)	3.36P_d (1.31 MPa)

PARAMETRIC EVALUATION

This section presents a parametric evaluation of the internal pressure capacity of a PCCV based on the previously detailed deterministic and probabilistic approaches, and focuses on influences of levels of prestressing and usage of fiber reinforced concrete (FRC). The level of prestressing refers to the ratio of the internal load offset by prestressing to the postulated design pressure (P_d), denoted as X in ASME BPVC III-2 Code Commentary (Figure 6(a)). PCCVs are typically designed for a value of X = 1.2~1.5 to remain in the elastic phase under design basis loading, but long-term effects from creep and shrinkage of concrete and stress relaxation of prestressing steel may degrade tendon force over the operational life span. Figure 6(b) depicts the radial displacement of the 1:4 scale PCCV model for X = 0.9, 1.2, 1.5, and 1.8.

FRC is defined as a composite with a concrete matrix reinforced by randomly oriented, dispersed fibers, whose addition provides improvements in aspects such as strength, ductility, and toughness (Naaman 2017). In the context of severe accidents where tensile forces are the primary sectional loads, the contribution of conventional concrete towards load capacity tends to be insignificant. On the other hand, FRC exhibits meaningful tensile post-peak strength and strain capacity via fiber bridging mechanisms, and this likely translates to the sectional response of a PCCV through tension stiffening. Choun et al. (2015) conducted uniaxial material tests and derived constitutive models for mixes of polyamide FRC (PFRC) and steel FRC (SFRC) to use for detailed PCCV analyses (Figure 7(a)). Figures 6(b), (c), and (d) depict the response of the PCCV model according to the usage of FRC and consideration of tension stiffening in conventional concrete, with levels of prestressing set as X = 0.9, 1.2, and 1.5. The internal pressure capacities according to the tendon and liner failure criteria of 0.8% and 0.4% are also shown, as well as the ratio of pressure capacity to that of the brittle tensile model assumed in previous sections.

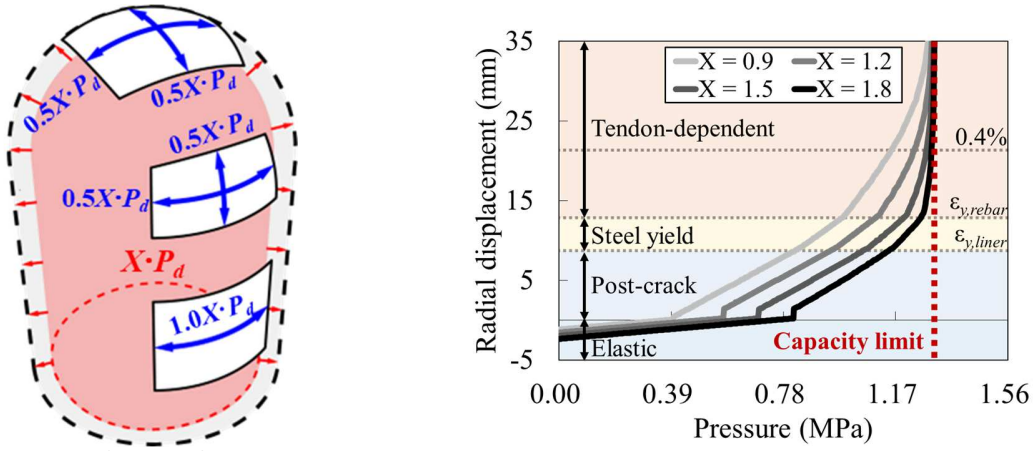

(a) Concept of level of prestressing (b) Parametric evaluation

Figure 6. Deterministic evaluation of internal pressure capacity according to level of prestressing

Figure 8 shows probabilities of failure according to usage of FRC for X = 0.9 and 1.5, where the liner peak strain criteria of 9% and 20% are assumed. The following observations are made from the deterministic and probabilistic parametric evaluations:

- Figure 6(b) indicates that increasing the levels of prestressing delays cracking of concrete and yielding of liner and reinforcing steel, increasing internal pressure capacity in terms of the 0.4% strain criteria, but not beyond an ultimate capacity limit. It should be noted that if yielding of liner and rebar is delayed to be concurrent with yielding in prestressing steel, the PCCV structure may show an abrupt shift towards the plastic phase, and functional and structural failures could potentially overlap. Conversely, it should also be considered that the analytical data by Dameron et al. (2003) in Figures 3(b) and (d) exhibits a marginal increase in capacity after global yield not captured in SCM, which would contribute towards functional failure occurring prior to structural failure.
- In Figures 7(b), (c), and (d), the implementation of tension stiffening smooths out the discontinuity previously observed at concrete cracking, but the internal pressure capacity for 0.4% global strain is not affected because stiffening effects would diminish at that strain level. Utilizing PFRC or SFRC bolsters the post-cracking and steel yield phases to roughly match the shapes of the constitutive laws. The graphs are still bound by the ultimate capacity limit, although the capacities are slightly increased due to residual stress in the FRC at failure strain.
- The internal pressure capacity values presented in Figures 7(b), (c), and (d) also show that the liner failure criteria of 0.4% only governs for X = 0.9, and average tendon strain criteria of 0.8% starts to govern for X = 1.2 and 1.5 due to the heightened initial strain. Due to the shift in governing strain criterion, the effectiveness of utilizing SFRC and PFRC over normal concrete is slightly diminished in the X = 0.9 ~1.2 range, from 5.7% and 1.9% to 5.5% and 1.8%, respectively. However, the effectiveness increases in the X = 1.2 ~1.5 range to 9.3% and 6.5% for SFRC and PFRC.
- In Figures 8(a) and (b), probabilistic curves for the 20% strain criterion roughly mirror deterministic curves near the capacity limit and those for the 9% strain criterion mirror curves near the post-cracking and steel yield phases, which is in line with observations in the previous section. Increasing the levels of prestressing offsets probability curves to the right, but a threshold pressure is observed similar to the deterministic curves, above which the probability of failure assuredly nears 100%. This is because the methodology essentially operates by assigning probabilistic modifiers to a deterministic peak strain (Figure 5(a)), resulting in the ultimate capacity limit being fixed deterministically.

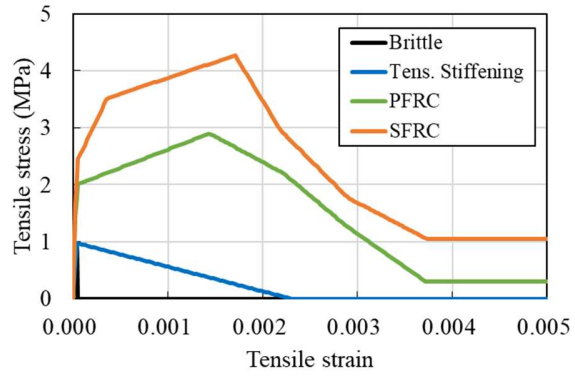

(a) Assumed tensile constitutive laws (Choun and Park 2015)

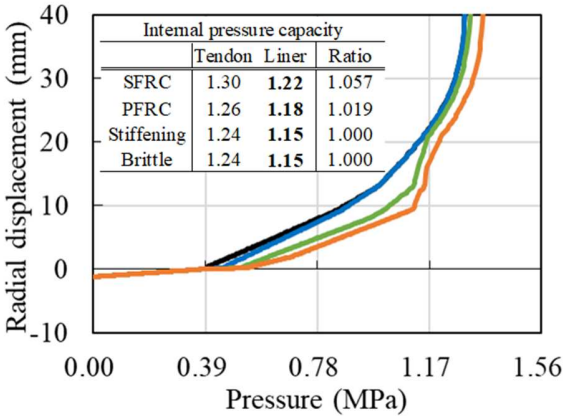

(b) X = 0.9

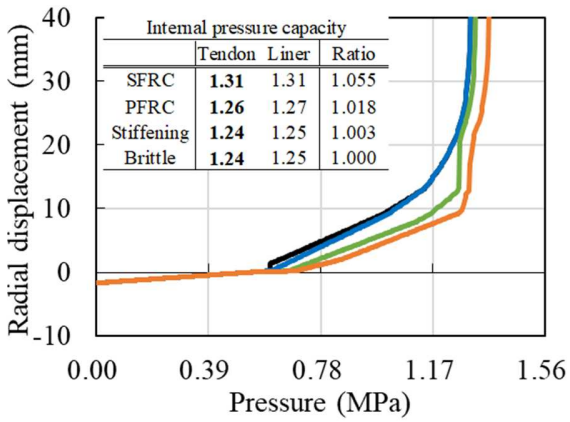

(c) X = 1.2

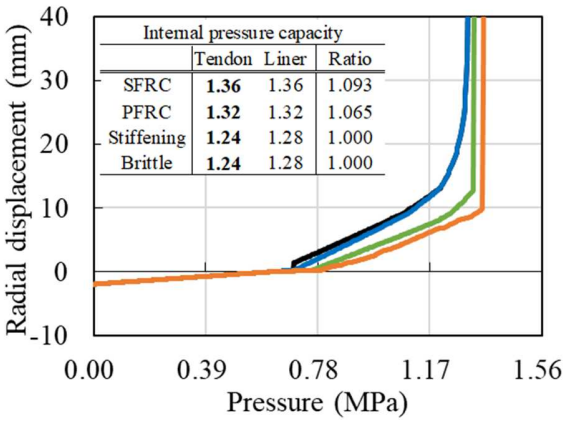

(d) X = 1.5

Figure 7. Deterministic evaluation of internal pressure capacity according to FRC usage

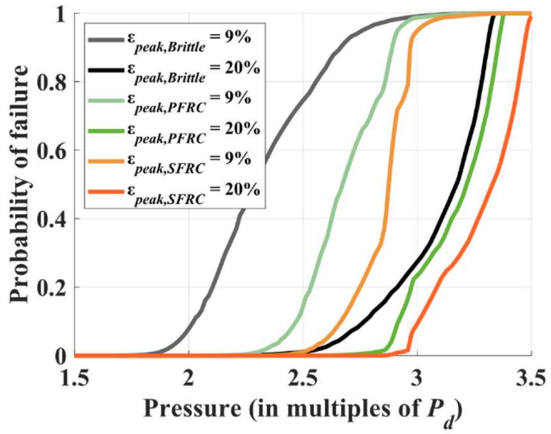

(a) X = 0.9

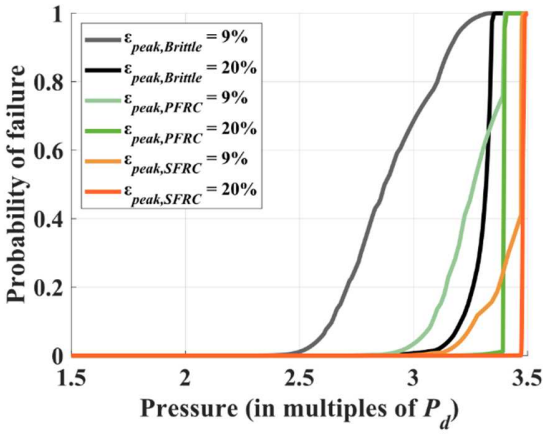

(b) X = 1.5

Figure 8. Probabilistic parametric evaluation of PCCV internal pressure capacity

CONCLUSION

This study investigates the internal pressure capacity of a 1:4 scale PCCV model by employing a sectional analysis methodology, combining deterministic and probabilistic approaches to assess the impact of design factors such as levels of prestressing and usage of fiber reinforced concrete. While this methodology has limitations in generalizing across the diverse array of PCCV designs and their intricacies, it provides insights for parametric trends and serves as a preliminary tool to guide more specific and comprehensive investigations. Future avenues of research could encompass the consideration of post-yield stress redistribution, the refinement of the EPRI methodology, or the exploration of biaxial and size effects in the implementation of fiber reinforced concrete.

ACKNOWLEDGEMENT

This work was supported by the Nuclear Safety Research Program through the Korea Foundation of Nuclear Safety (KoFONS) using the financial resource granted by the Nuclear Safety and Security Commission (NSSC) of the Republic of Korea (No. 2203024). Additionally, this work was supported using the financial resource granted by ASME Standards Technology, LLC (ASME ST, LLC) of the United States of America (Project 197).

REFERENCE

Choun, Y. and Park, H. (2015). “Containment Performance Evaluation of Prestressed Concrete Containment Vessels with Fiber Reinforcement”, *Nuclear Engineering and Technology*, 47(7), pp. 884-894

Dameron, R., Zhang, L., Rashid, Y., and Vargas, M. (2000). “Pretest Analysis of a 1:4-Scale Prestressed Concrete Containment Vessel Model,” NUREG/CR-6685, SAND2000-2093, U.S. Nuclear Regulatory Commission, USA.

Dameron, R., Hansen, B., Parker, D., and Rashid, Y. (2003). “Posttest Analysis of the NUPEC/NRC 1:4 Scale Prestressed Concrete Containment Vessel Model,” NUREG/CR-6809, SAND2003-0839P, ANA-01-0330, U.S. Nuclear Regulatory Commission, USA.

Heitman, L., Jones, C., Dameron, R., Graves, H., and Sircar, M. (2014). “Phase Two of Standard Problem Exercise #3 to Determine Containment Vessel Performance under Severe Accident Conditions,” SAND2013-2650P, Sandia National Laboratories, USA.

Hessheimer, M., Klamerus, E., Lambert, L., Rightley, G., Dameron, R. (2003). “Overpressurization Test of a 1:4-Scale Prestressed Concrete Containment Vessel Model,” NUREG/CR-6810, SAND2003-0840P, U.S. Nuclear Regulatory Commission, USA.

Hessheimer, M., and Dameron, R. (2006). “Containment Integrity Research at Sandia National Laboratories,” NUREG/CR-6906, SAND2006-2274P, Sandia National Laboratories, USA.

Johnston, T., Hovis, B., Jovall, O., and Munshi, J. (2016). “Commentary on Article CC-3000 Design,” ASME Press, USA.

Naaman, A. (2017). “Fiber Reinforced Cement and Concrete Composites,” Technopress 3000, USA.

NEA (2005). “International Standard Problem No. 48: Containment Capacity – Synthesis Report,” OECD Nuclear Energy Agency, France.

NRC (2008). “Draft Regulatory Guide DG-1203, Containment Performance for Pressure Loads,” U.S. Nuclear Regulatory Commission, USA.

NRC (2010). “Regulatory Guide 1.216, Containment Structural Integrity Evaluation for Internal Pressure Loadings Above Design-Basis Pressure,” U.S. Nuclear Regulatory Commission, USA.

Tang, H., Dameron, R., and Rashid, Y. (1995). “Probabilistic Evaluation of Concrete Containment Capacity for Beyond Design Basis Internal Pressures,” *Nuclear Engineering and Design*, 157(3), pp. 455-467.